Grant Agreement No: 101004761

AIDAinnova

Advancement and Innovation for Detectors at Accelerators

Horizon 2020 Research Infrastructures project AIDAINNOVA

DELIVERABLE REPORT

Report on performance of radiation-hard DMAPS

DELIVERABLE: D5.3

Document identifier:	AIDAinnova-D5.3
Due date of deliverable:	End of Month 36 (March 2024)
Report release date:	30/04/2024
Work package:	WP5: Depleted Monolithic Active Pixel Sensors
Lead beneficiary:	UBonn
Document status:	Final

Abstract:

This deliverable report summarizes the performance studies of the Depleted Monolithic Active Pixel Sensors (DMAPS) prototypes, which primarily target excellent radiation tolerance (radiation-hard), carried out in the project. Each effort resulted in one or more publications highlighted in the report.

For more information on AIDAinnova, its partners and contributors please see http://aidainnova.web.cern.ch/

The Advancement and Innovation for Detectors at Accelerators (AIDAinnova) project has received funding from the European Union's Horizon 2020 Research and Innovation programme under Grant Agreement no. 101004761. AIDAinnova began in April 2021 and will run for 4 years.

Delivery Slip

	Name	**Partner**	**Date**
Authored by	F. Huegging N. Wermes S. Grinstein	Ubonn, IFAE	25/04/2024
Reviewed by	Daniela Bortoletto [Deputy Scientific coordinator]	UOXF	30/04/2024
Approved by	Daniela Bortoletto [Deputy Scientific coordinator] Steering Committee	UOXF	30/04/2024

TABLE OF CONTENTS

Executive summary

The production and initial tests of several Depleted Monolithic Active Pixel Sensors (DMAPS) using CMOS technologies that primarily target excellent high radiation tolerance (radiation-hard) have been successfully carried out and included in the AIDAinnova Milestone report MS20 [1]. This report presents the characterization of these prototypes which resulted in one or more publications (highlighted in the report).

The LF-Monopix2 is a full-size, mature device, that is being characterized in the context of the AIDAinnova WP5 activities. The encouraging results obtained before and after irradiation are summarized below [3, 4, 5].

The RD50-MPW 2/3/4 development is a similar approach in the same technology. Characterizations obtained in the context of AIDAinnova WP5 activities revealed that this approach still has not fulfilled its promises. Several severe bug fixes were necessary, but with the latest chip iteration, a working chip is available, which can be studied now before and after irradiation [6, 7, 8].

These activities constitute unique advances in bringing the Monolithic DMAPS detectors to the next generation of High Energy Physics experiments.

1 INTRODUCTION

Depleted Monolithic Active Pixel Detectors (DMAPS) are a key technology for the AIDAinnova project. They constitute the most interesting new direction of pixel detector development and are a fundamental approach for present and planned accelerator experiments.

The WP5 activities branch into two main lines, one focusing on high granularity devices, targeting above all high position resolution, the other targeting foremost high radiation hardness. The production and initial tests of several radiation-hard DMAPS prototypes are documented in the AIDAinnova Milestone report MS20 [1]. The current Deliverable Report concentrates on the performance of prototypes of DMAPS devices that target radiation hardness. This Report includes the characterization of the following prototype devices:

1. LF-Monopix2 sensors in 150 nm CMOS technology is a mature large-size prototype that implements a full readout architecture.
2. RD50-MPW2/3/4, also in 150 nm technology, is a recent development of a somewhat more exploratory endeavour.

Each section below summarizes the main results of these efforts, followed by the conclusions and outlook.

2 RADIATION HARD DMAPS PROTOTYPE DEVELOPMENT

The development of Depleted Monolithic Active Pixel sensors has followed so far essentially two generally different design approaches (Fig. 2.1): (a) large electrode design and (b) small electrode design. While within AIDAinnova (a) is the prime approach for high radiation hardness, (b) targets primarily high granularity, i.e. small pixels, low-noise and low-power operation, albeit with good radiation tolerance. Development of designs (a) is the theme of this report.

The large electrode design benefits charge collection, making, in principle, the approach intrinsically more radiation-hard compared to small electrode designs, which is critical for specific applications, particularly in inner layers of tracking detectors in hadron collider experiments. On the downside, large electrodes result in a larger capacitance at the input of the pre-amplifiers, resulting in larger noise and power consumption as well as slower timing. Therefore, the development focuses on achieving full charge collection after irradiation while ensuring a large signal-to-noise ratio for high hit-detection efficiency.

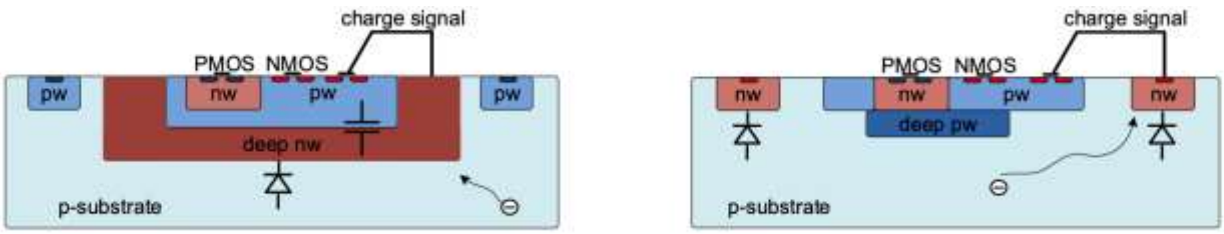

Fig. 2.1 Two approaches for DMAPS: (a) large electrode cell design, (b) small electrode cell design.

3 PROTOTYPE LF-MONOPIX2 IN 150 NM TECHNOLOGY

The Monopix chip line includes prototypes in the TowerJazz 180 nm and LFoundry 150 nm technologies. LF-Monopix2 chip has a size of 1×2 cm^2 and a pixel pitch of 50×150 µm^2 (see Fig. 3.1). Its predecessor was LF-Monopix1 [2]. The pixel matrix takes up 82% of the chip area, the rest is occupied by guard rings, decoupling capacitors and peripheral circuitry at the top and bottom of the chip. Due to the smaller pixel size and hence reduced capacitance ($250 - 300$ fF) an improved signal-to-noise ratio and a better timing performance are expected. The large electrode approach should result in excellent charge collection after irradiation.

The matrix is divided into three main sub-matrices, including different charge-sensitive amplifier (CSA) designs. One of the sub-matrices is further subdivided into four regions with different CSA feedback capacitances (1.5 fF or 5.0 fF), local threshold tuning schemes (unidirectional or bidirectional) and pixel-level logic. The pixel design of LF-Monopix2 features rounded corners for reduction of the electric field on the edges, which, together with an optimized guard-ring design, improve the breakdown behaviour of the sensor. Wafers have successfully been thinned to 100 µm and backside-processed [3]. Proton irradiated samples up to a 1- MeV equivalent fluence of 2×10^{15} n_{eq}/cm^2 are available. The chips were not powered during the irradiation and annealed for 80 min at 60 °C afterwards.

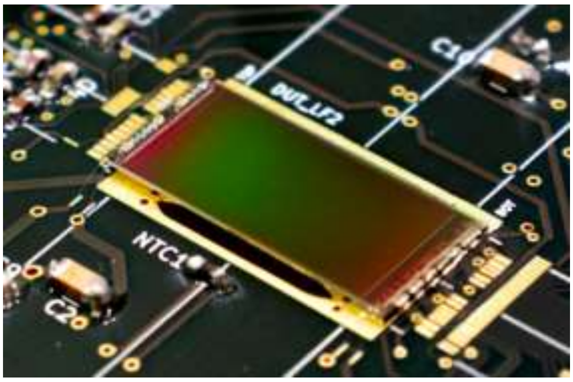

Figure 3.1: Photographs of successfully produced LF-Monopix2 mounted on a readout board.

Measurements in a controlled laboratory environment at -20 °C confirmed the functionality of LF-Monopix2 chips after irradiation. All irradiated samples were fully operational at their target fluence and could successfully be tuned to a typical mean threshold response of 2 ke⁻. Figure 3.2 displays the leakage current of the sensor as a function of the reverse bias voltage applied across different irradiation steps. For the non-irradiated sample, a breakdown voltage of 460V is observed [4]. To prevent damage to the chips, a maximum of 300 V bias voltage was applied to irradiated samples. After an irradiation of $1x10^{15}$ n_{eq}/cm^2, an increase in the leakage current of around 5 µA/cm² at 100 V bias voltage is observed.
The Equivalent Noise Charge (ENC) performance of the largest sub-matrix for LF-Monopix2 is depicted in Figure 3.3 for the different irradiation steps available. The larger leakage current after irradiation increases the ENC from 87 e^- in the non-irradiated case to 178 e^- after a fluence of $2x10^{15}$ n_{eq}/cm^2 [5]. Nevertheless, a threshold response of around 2 ke^- is still achievable after all irradiation steps.

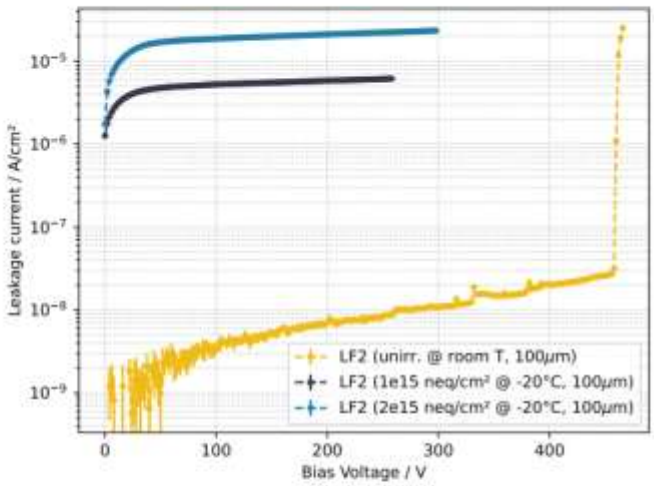

Figure 3.2: Leakage current of LF-Monopix2 at 0, 1, and 2 x 10^{15} MeV n_{eq}/cm^2 as a function of reversed bias voltage normalized to the sensitive sensor area.

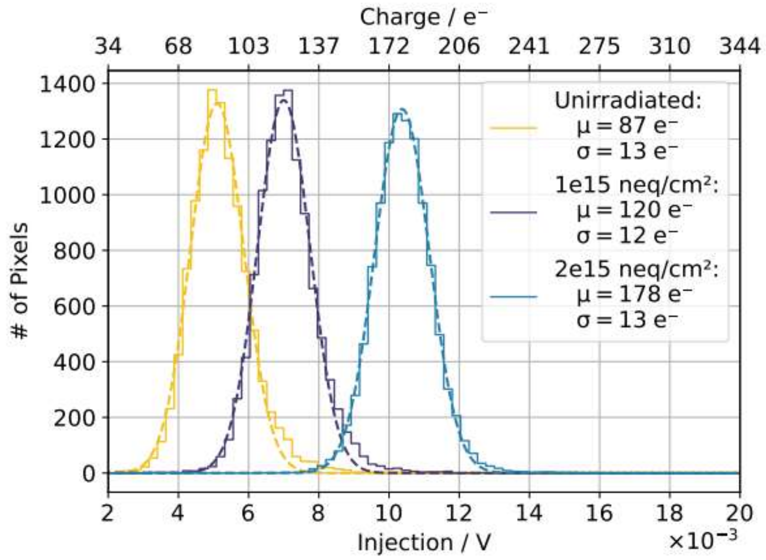

Figure 3.3: Comparison of ENC distribution of LF-Monopix2 at 0, 1, and 2 x 10^{15} MeV n_{eq}/cm² measured in a controlled laboratory environment at -20 °C

Beam test measurements were conducted at the DESY test beam facility utilizing a 5 GeV electron beam and standard EUDET-type beam telescope setup. All measurements were taken with a typical operational threshold of 2 ke⁻, while the irradiated samples had to be cooled to -20 °C during operation to compensate for the increase in leakage current. A comparison of the measured hit-detection efficiency between the different irradiation steps available is shown in Figure 3.4. Increasing the bias voltage improves the hit-detection efficiency until full depletion of the sensitive volume is reached. The reverse bias voltage needed to fully deplete a 100 µm thick sample increases from 15 V before irradiation to around 150 V after exposure to a fluence of 2x10^{15} n_{eq}/cm². Hit-detection efficiencies larger than 99.5 % were measured for all irradiation steps after full depletion of the sensitive volume [5].

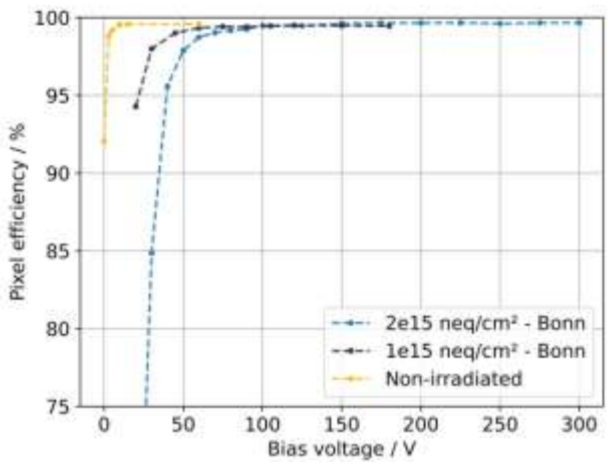

Figure 3.4: Comparison of the hit-detection efficiency of a 5 GeV electron beam as a function of the bias voltage for 0, 1, and 2 x 10^{15} MeV n_{eq}/cm². An increase in efficiency for larger bias voltages is visible until the full depletion of the sensitive volume is reached. For higher irradiation fluences, larger voltages are needed to reach the full depletion. All samples were operated with a mean threshold of around 2 ke⁻.

Additionally, the arrival time of hits in relation to the event is used to define an *in-time* efficiency corresponding to a 25 ns time window within which the detected hits must arrive. A projection of the measured *in-time* efficiency onto a 2x2 pixel array facilitates the study of the performance within a pixel. Figure 3.5 shows such a projection for an LF-Monopix2 sample irradiated to a fluence of 2x10^{15} n_{eq}/cm² and operated at 2 ke⁻ mean threshold and 150 V bias voltage. The measured mean *in-time* efficiency of 98.35% is above the initial design goal of 97% hit-detection efficiency within a 25 ns window required at a fluence of 1x10^{15} n_{eq}/cm². The drop in *in-time* efficiency at the pixel corner to 96.10% is explained by the reduction of the input signal due to charge sharing between neighbouring pixels. The *in-time* performance is further enhanced by increasing the signal gain by reducing the feedback capacitance from 5.0 fF to 1.5 fF. For the corresponding sub-matrix implemented in LF-Monopix2, efficiencies larger than 99% within a 25 ns time window were measured even after irradiation to 2x10^{15} n_{eq}/cm² [5].

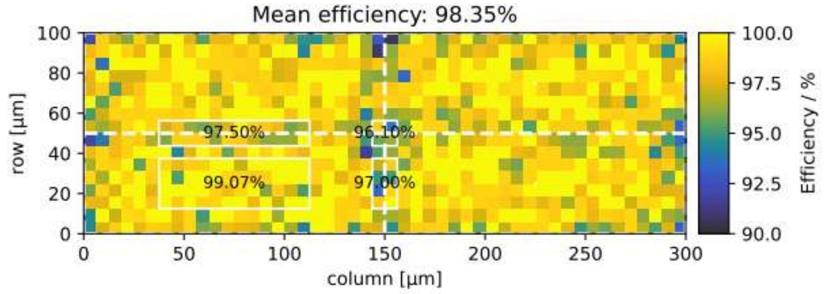

Figure 3.5: Mean in-time efficiency of 98.35% measured with a 2x10^{15} n_{eq}/cm² fluence irradiated LF-Monopix2 sensor at 150 V bias voltage and 2 ke⁻ thresholds. The results are projected onto a 2x2 pixel map to study the performance within a pixel. A drop of the in-time efficiency to 96.10% in the pixel corners is visible.

Since the performances after fluences of 2x10^{15} n_{eq}/cm² are very promising, irradiation of LF-Monopix2 to even higher fluences (3x10^{15} n_{eq}/cm²) is in preparation. Furthermore, an irradiation and measurement campaign up to a total ionizing dose of 100 MRad finished very recently. While the sample was still responsive and fully operational after the maximum dose, a detailed analysis of the results is still ongoing.

4 PROTOTYPE RD50-MPW2, 3 AND 4 IN 150 NM TECHNOLOGY

Another effort to develop radiation-hard devices was launched after the LF-Monopix approach. The RD50-MPW2 chip [5], fabricated in the framework of AIDAinnova, followed the MPW1 chip, which suffered from a large leakage current. To understand the high current, the MPW2 chip implements a smaller, very simple chip structure with a guard ring frame at the edge. The chip avoided specific post-processing filling layers that involve conductive material. The chip has 8 rows x 8 columns of 60 µm x 60 µm pixels with analogue readout only (see Fig. 4.1).

The RD50-MPW2 has several design limitations, such as the small number of rows and columns of the pixel matrix, the lack of digital readout electronics to identify events and a very simple peripheral readout that makes certain types of measurements too slow or impossible. Therefore, the MPW2 chip was closely followed by the RD50-MPW3 [7], which overcomes the limitations of its predecessor by extending the number of pixels in the matrix (64 columns x 64 rows), incorporating in the pixel area digital readout electronics based on the column drain architecture, and adding optimized peripheral readout electronics for effective pixel configuration.

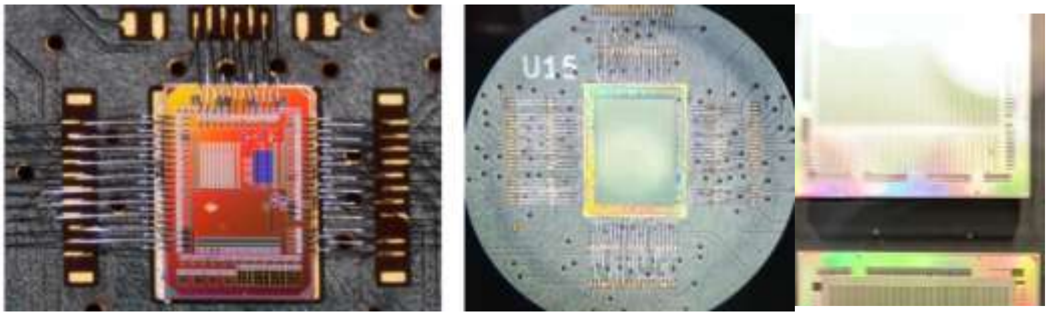

Figure 4.1: Photographs of produced RD50-MPW2 (left) and RD50-MPW3 (middle) chips mounted on boards for testing as well as MPW4 bare chip (right).

The MPW3 devices processed on 2 kΩcm wafers were received in July 2022. Initial tests showed that the chip was operational but suffered from a very high pixel ENC, an order of magnitude larger than the expected signal of ~2000 e^-. This noise was traced back to a cross-coupling of the digital periphery to the analogue part of the pixel matrix. Consequently, poor noise behaviour is much more pronounced in the lower part of the matrix, which is closer to the periphery. Thus, the chip is barely functional since thresholds must be increased to values higher than the noise, resulting in very poor hit reconstruction efficiencies in test beam operation. Moreover, the breakdown voltage of the chips, which is about 150 V, is lower than the target.

Both problems are addressed by another chip submission with a few bug fixes, including an improved guard ring design and, most importantly, a redesign of the digital readout periphery. Post-layout simulation suggested that separating the power and ground lines between the pixel matrix and the periphery should avoid the cross-coupling yielding high pixel noise. This MPW4 chip was submitted in 2023, and the first tests on 3 kΩcm wafers in early 2024 showed promising results. The breakdown voltage for chips on backside processed wafers increased to at least 400 to 600 V, and the pixel ENC dropped to about 200 e-, as seen in Fig. 4.2.

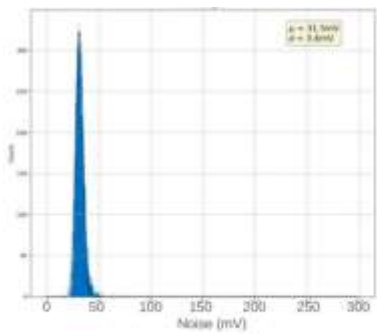

Figure 4.2: Noise level of the RD50-MPW4 devices, indicating that the coupling with the digital part of the chip is solved in this last iteration. The pixel is given here in mV, and the measured 31.5 mV corresponds to about 200 e^- ENC.

The next steps of this project include detailed tests of the chip before and after irradiation to several 10^{15} MeV n_{eq}/cm^2 in laboratory and test beam environments. It is expected that the results of these studies will be available before the end of the project and will be reported in later project reports.

5 CONCLUSIONS AND FUTURE PLANS

The results of the characterization of radiation-hard DMAPS prototypes LF-Monopix2 and RD50-MPW 2/3/4 were presented. The LF-Monopix2 large-size devices offer excellent results in terms of operation before and after irradiation to $2x10^{15}$ n_{eq}/cm^2. This proves with experiment-ready devices that radiation-tolerant DMAPS fulfilling the demanding requirements for operation in proton collider vertex detectors are feasible. Further performance results at even higher irradiation fluence and TID doses will follow.
The RD50-MPW2/3/4 development on the other hand is not at the same maturity level. Several design changes and chip iterations were necessary during the last years to fix nearly fatal chip problems. Thus, the detailed performance characterization before and after irradiation was not yet possible. However, with the last iteration of RD50-MPW4 we expect to obtain these results before the end of the project.

6 REFERENCES

[1] N. Wermes, F. Huegging and S. Grinstein, "Radiation Hard Prototype Fabrication", AIDAinnova Milestone report, https://zenodo.org/records/7920666.

[2] P. Rymazewski et al., "Development of depleted monolithic pixel sensors in 150 nm CMOS technology for the ATLAS inner tracker upgrade", PoS, TWEPP-17 (2018), p. 045, doi:10.22323/1.313.0045

[3] J. Dingfelder, et al., "Progress in DMAPS developments and first tests of the Monopix2 chips in 150 nm LFoundry and 180 nm TowerJazz technology", VERTEX 21. doi:10.1016/j.nima.2022.166747

[4] I. Caicedo, et al., "Improvement in the Design and Performance of the Monopix2 Reticle-Scale DMAPS", VERTEX 22, (in press)

[5] L. Schall, et al., "Test-beam performance of proton-irradiated, large-scale depleted monolithic active pixel sensors in 150 nm CMOS technology", VERTEX 23. doi:10.22323/1.448.0043

[6] E. Vilella et al., "Development of high voltage-CMOS sensors within the CERN-RD50 collaboration", Vol 1034 (2022), 166826. doi:10.1016/j.nima.2022.166826

[7] P. Sieberer et al., "Design and characterization of depleted monolithic active pixel sensors within the RD50 collaboration", Vol 1039 (2022), 167020. doi:10.1016/j.nima.2022.167020

[8] B. Wade et al., "Edge-TCT evaluation of high voltage-CMOS test structures with unprecedented breakdown voltage for high radiation tolerance", JINST 17 C12017 (2022). doi:10.1088/1748-0221/17/12/C12017

NOTE: for a full list of the AIDAinnova WP5 publications, please see the following link: https://zenodo.org/communities/aidainnova-project/search?page=1&size=20&keywords=WP5.

ANNEX: GLOSSARY

Acronym	**Definition**
DMAPS	Depleted Monolithic Active Pixel Sensors